

# Dynamic Patterns of Histone Methylation Are Associated with Ontogenic Expression of the *Cyp3a* Genes during Mouse Liver Maturation<sup>S</sup>

Ye Li, Yue Cui, Steven N. Hart, Curtis D. Klaassen, and Xiao-bo Zhong

Department of Pharmacology, Toxicology, and Therapeutics, the University of Kansas Medical Center, Kansas City, Kansas

Received October 22, 2008; accepted February 2, 2009

## ABSTRACT

Human cytochrome P450 3A (CYP3A) members are major drug-metabolizing enzymes in the liver. Two genes, *CYP3A4* and *CYP3A7*, exhibit a developmental switch in gene expression during liver maturation. *CYP3A4* is mainly expressed in adults, whereas *CYP3A7* is dominantly expressed during the fetal and neonatal stages. Their ontogenic expression results in developmentally related changes in the capacity to metabolize endogenous and exogenous compounds. Thus, it is desirable to understand the mechanisms controlling the developmental switch. Mice also exhibit a developmental switch between *Cyp3a16* (neonatal isoform) and *Cyp3a11* (adult isoform) and may serve as a model to study the mechanisms controlling the developmental switch. Because the epigenetic code (e.g., DNA methylation and histone modifications) is implicated in regulating gene expression and cellular differentiation during develop-

ment, the current study determined the status of DNA methylation, histone-3-lysine-4 dimethylation (H3K4me2) and histone-3-lysine-27 trimethylation (H3K27me3) around the mouse *Cyp3a* locus at various developmental ages from prenatal, through neonatal, to young adult. DNA was not hypermethylated in the *Cyp3a* locus at any age. However, increases in *Cyp3a16* expression in neonatal livers and *Cyp3a11* in adult livers were associated with increases of H3K4me2. Suppression of *Cyp3a16* expression in adult livers coincided with decreases of H3K4me2 and increases of H3K27me3 around *Cyp3a16*. In conclusion, histone modifications of H3K4me2 and H3K27me3 are dynamically changed in a locus-specific manner along the *Cyp3a* locus. Developmental switch between *Cyp3a11* and *Cyp3a16* gene expression seems to be due to dynamic changes of histone modifications during postnatal liver maturation.

Human cytochrome P450 3A (CYP3A) subfamily members are major drug-metabolizing enzymes, responsible for metabolizing more than 50% of prescribed drugs and some endogenous compounds (Wilkinson, 2005). Two members in this subfamily, CYP3A4 and CYP3A7, are expressed in liver with distinct ontogenic patterns during liver maturation (Schuetz et al., 1994; Lacroix et al., 1997; Stevens et al., 2003; Leeder et al., 2005). *CYP3A7* is predominantly expressed in prenatal and neonatal livers but also expressed in approximately 10% of adult livers because of genetic polymorphisms and/or unknown mechanisms (Sim et al., 2005). CYP3A4 is the major adult hepatic CYP3A isoform. A developmental switch in

gene expression between *CYP3A7* and *CYP3A4* occurs during the first 1 to 2 years after birth.

Although highly similar in sequence and structure, CYP3A4 and CYP3A7 differ in their capacity and specificity for the metabolism of xenobiotics and endobiotics (Williams et al., 2002). Considerable differences in the ontogenic gene expression and substrate specificities among these isoforms contribute to differences in drug metabolism between children and adults (Stevens, 2006; Hines, 2008). However, the mechanisms that control the developmental switch of gene expression have not been determined.

A developmental switch has also been observed in the *Cyp3a* genes in mouse liver (Itoh et al., 1997; Nakayama et al., 2001; Hart et al., 2009). Comparison of the genomic organization between the human *CYP3A* cluster and the mouse *Cyp3a* locus, which is illustrated in Fig. 1, shows the high similarities of DNA and protein sequences between human CYP3A and mouse *Cyp3a* isoforms. Mouse *Cyp3a* genes are located in a highly conserved area at the distal end

This work was supported by the National Institutes of Health National Center for Research Resources [Grant 5P20-RR021940].

Article, publication date, and citation information can be found at <http://molpharm.aspetjournals.org>.

doi:10.1124/mol.108.052993.

<sup>S</sup> The online version of this article (available at <http://molpharm.aspetjournals.org>) contains supplemental material.

**ABBREVIATIONS:** *CYP3A4*, human cytochrome P450, family 3, subfamily A, polypeptide 4 gene; *Cyp3a11*, mouse cytochrome P450, family 3, subfamily a, polypeptide 11 gene; *Cyp3a16*, mouse cytochrome P450, family 3, subfamily a, polypeptide 16 gene; DNAm, DNA methylation; H3K4me2, histone 3 lysine 4 dimethylation; H3K27me3, histone 3 lysine 27 trimethylation; TSS, transcription start sites; ChIP, chromatin immunoprecipitation; bp, base pair; Mb, megabase; PCR, polymerase chain reaction.

of chromosome 5. Adjacent 5' and 3' domains of the mouse *Cyp3a* locus are also highly conserved between mice and humans. The adjacent 5' domain is a gene-dense area in mice, consisting of 13 genes in ~200 kilobases. Some of the genes are housekeeping genes, such as zinc finger protein genes (e.g., *Zfp498*, *Zfp655*, *Zkscan14*), and ATP synthase (*Atp5j2*) (Fig. 1). This domain shares synteny to the 5'-adjacent domain of the human *CYP3A* locus on chromosome 7. In contrast, the adjacent 3' domain (~180 kilobases) in mice contains ring finger protein 6 (*Rnf6*) and cyclin-dependent kinase 8 (*Cdk8*) genes, which shares synteny to a chromosome region on human chromosome 13. In addition to being homologous in DNA and protein sequences to the human *CYP3A* isoforms, mouse *Cyp3a11* and *Cyp3a16* also mimic a developmental switch as human *CYP3A4* and *CYP3A7* (Hart et al., 2009). The switch between the neonatal isoform of *Cyp3a16* and the adult isoform of *Cyp3a11* occurs between days 5 and 20 after birth. Understanding the mechanisms controlling the developmental switch of the mouse *Cyp3a* genes may provide a clue to the human *CYP3A* switch.

Recent studies have shown that developmentally programmed gene expression patterns are associated with dynamic epigenetic modifications (Kiefer, 2007; Reik, 2007). DNA methylation and histone modifications are the two important reversible epigenetic modifications that influence gene transcription during development. DNA methylation can either directly interfere with binding of transcriptional factors to their recognition sites or indirectly influence the

recruitment of corepressors by methyl-CpG binding domain proteins (Nan et al., 1998). It has been shown that DNA methylation is essential for normal development (Bird, 2002) and also implicated in many pathologies including cancer, imprinting disorders, and repeat-instability diseases (Robertson, 2005; Esteller, 2007; Feinberg, 2007). Post-translational modifications in the N-terminal tails of histones result in the alteration of DNA-histone interactions within or between nucleosomes and thus affect higher-order chromatin structures, influencing the ability of a gene to be expressed (Kouzarides, 2007; Bártová et al., 2008). Methylation at histone 3 lysine 27 (H3K27me3 and H3K27me2) is associated with repression of gene transcription, whereas methylation at histone 3 lysine 4 (H3K4me3, H3K4me2, and H3K4me1) is linked to activation of gene transcription (Heintzman et al., 2007; Wang et al., 2008). Among the H3K4me1, H3K4me2, and H3K4me3, H3K4me3 is enriched more frequently around transcription start sites (TSS) of genes; in contrast, H3K4me2 and H3K4me1 occur over a larger area, such as promoters, enhancers, and long-range regulatory elements (Heintzman et al., 2007). Furthermore, methylation at H3K27 and H3K4 can act as bivalent switches to turn on/off their associated genes during development (Lan et al., 2007; Swigut and Wysocka, 2007). Therefore, the current study selected H3K4me2 and H3K27me3 as the histone modification markers, together with DNA methylation, to observe effects of epigenetic modifications on the regulation of the *Cyp3a* gene expression in mouse livers during development.

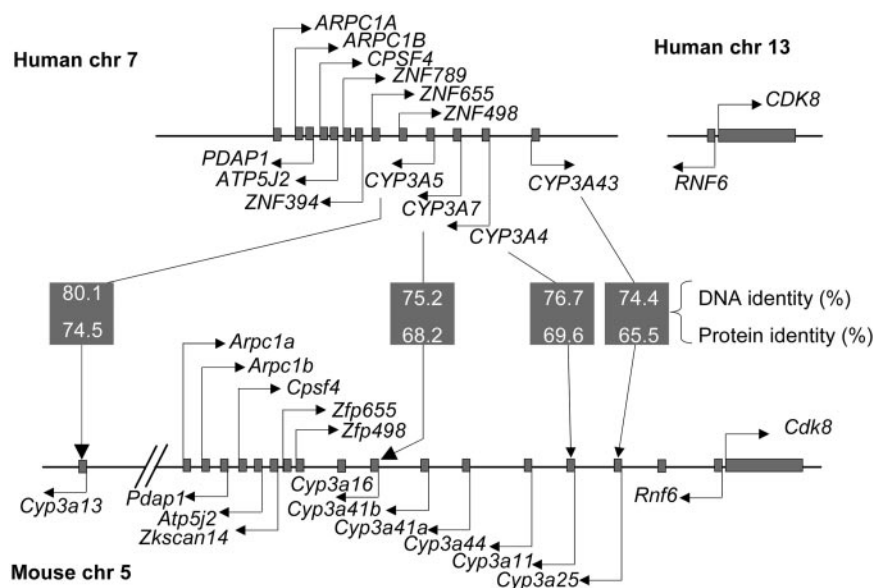


**Fig. 1.** Comparison of genomic organization between the mouse *Cyp3a* and human *CYP3A* gene clusters and their adjacent 5' and 3' domains. Based on the University of California Santa Cruz Genome Browser Mouse February 2006 Assembly, the mouse chromosome 5 contains two parts from left to right: part 1 from nucleotide position of 138,112,721 to 138,161,405 containing the *Cyp3a13* gene; and part 2 from 145,327,396 to 146,617,044 containing the *Cyp3a* locus and its 5' and 3' adjacent domains. In Human March 2006 Assembly, two syntenic regions are located at chromosome 7 from 98,751,446 to 99,312,109 and chromosome 13 from 25,674,905 to 25,886,569. *Arpc1a*, mouse actin-related protein complex subunit a gene; *ARPC1A*, human actin-related protein complex subunit A gene; *Arpc1b*, mouse actin-related protein complex subunit b gene; *ARPC1B*, human actin-related protein complex subunit B gene; *Atp5j2*, mouse ATP synthase, H<sup>+</sup> transporting, mitochondrial F0 complex, subunit f, isoform 2 gene; *ATP5J2*, human ATP synthase, H<sup>+</sup> transporting, mitochondrial F0 complex, subunit F, isoform 2 gene; *Cdk8*, mouse cyclin-dependent kinase 8 gene; *Cpsf4*, mouse cleavage and polyadenylation-specific factor 4 gene; *CPSF4*, human cleavage and polyadenylation-specific factor 4 gene; *Pdap1*, mouse platelet-derived growth factor A-associated protein 1 gene; *PDAP1*, human platelet-derived growth factor A-associated protein 1 gene; *Rnf6*, mouse ring finger protein 6 gene; *RNF6*, human ring finger protein 6 gene; *Zfp99*, *Zfp498*, and *Zfp655*, mouse zinc finger protein 99, 498, and 655 genes, respectively; *ZNF394*, *ZNF498*, *ZNF655*, and *ZNF789*, human zinc finger protein 394, 498, 655, and 789 genes, respectively.

## Materials and Methods

**Animals.** Eight-week-old C57BL/6 breeding pairs of mice were purchased from Charles River Laboratories (Wilmington, MA). Mice were housed according to the American Animal Association Laboratory Animal Care guidelines and were bred under standard conditions in the Lab Animal Resources Facility at the University of Kansas Medical Center. The use of these animals was approved by the Institutional Animal Care and Use Committee. Breeding pairs were set up at 4:00 PM and separated at 8:00 AM the following day. The body weights of female mice were recorded each day to determine pregnancy status. Livers from offspring were collected at the following four ages: days -2 (gestational day 17), 1, 5, and 45, which represent developmental stages of prenatal (day -2), neonatal (day 1 and 5), and young adults (day 45) during liver maturation. Because of the difficulty in distinguishing gender from day -2 to day 5 mice and no gender differentiation in these ages, livers from at least five offspring of the same litters were pooled at each age to achieve the desired amount of tissue (200–300 mg). Only male mice for the young adult group (day 45) were selected in this study to eliminate gender difference. Livers were frozen immediately in liquid nitrogen and stored at -80°C.

**ChIP-on-Chip Assay.** DNA methylation and histone modifications of H3K4me2 and H3K27me3 in livers of mice at days -2 (gestation day 17), 1, 5, and 45 were determined by Genpathway (San Diego, CA) using the ChIP-on-chip assays with the Affymetrix GeneChip Mouse Tiling 2.0R E arrays (Affymetrix, Santa Clara, CA), which contain more than 6.5 million perfectly matched tiling probes to mouse chromosomes 5, 12, and 15. The probes were tiled at an average resolution of 35 base pairs, as measured from the central position of adjacent 25-mer oligonucleotides, leaving a gap of approximately 10 bp between two probes. Repetitive elements and identical sequences within gene families were removed from the arrays to avoid cross-hybridization of target DNA fragments to multiple genomic areas; therefore, some genomic areas might have hybridization signal gaps.

**DNA Methylation.** Genomic DNA from the liver tissues was isolated by a ChargeSwitch gDNA Mini Tissue Kit (Invitrogen, Carlsbad, CA) and sonicated to an average length of 300 to 500 bp. An antibody against 5-methyl-cytosine (ab51552; Abcam Inc. Cambridge, MA) was used for immunoprecipitation of methylated DNA fragments as described previously (Pröll et al., 2006; Zhang et al., 2006). The purified ChIP-enriched fragments were amplified by using Sigma GenomePlex Kit (Sigma-Aldrich, St. Louis, MO) according to the manufacturer's protocol (O'Geen et al., 2006). The amplified DNAs were purified, quantified, and tested by quantitative PCR at the same genomic regions as the original immunoprecipitated DNA to assess the quality of the amplification reactions. The amplified DNAs were fragmented, labeled with the DNA Terminal Labeling Kit according to the standard Affymetrix protocol, and hybridized to arrays. Total genomic DNA without immunoprecipitation was also hybridized to a single array and served as a background control (input) for all immunoprecipitated DNA. Arrays were washed and scanned by a GeneChip HT Array Plate Scanner according to Affymetrix's standard procedures.

**Histone Modification.** Likewise, histone modification profiles of H3K4me2 and H3K27me3 were established by using a protocol similar to that of DNA methylation but with polyclonal antibodies of Millipore 07-030 (anti-H3K4me2) and 07-449 (anti-H3K27me3), respectively. In brief, frozen liver tissues were fixed with 1% formaldehyde in phosphate-buffered saline containing 1 mM dithiothreitol at room temperature for 15 min and quenched with 0.125 M glycine for another 5 min. The tissues were disaggregated with a Tissue Tearor (BioSpec Products, Bartlesville, OK), and chromatin was isolated by adding radioimmunoprecipitation assay buffer supplemented with 1 mM dithiothreitol, 1 mM phenylmethylsulfonyl fluoride, and 10 mM EDTA, followed by disruption with a Dounce homogenizer. Lysates were sonicated, and the DNA was sheared to

an average length of 300 to 500 bp. Genomic DNA (input) was prepared by treating aliquots of chromatin with RNase and proteinase K followed by phenol and chloroform extractions and ethanol precipitation. An aliquot of chromatin (~30 µg) was used to perform ChIP as described previously (Wang et al., 2008). ChIP and input DNAs were amplified by whole-genome amplification using the GenomePlex Whole-Genome Amplification Kit (Sigma-Aldrich). Fragmentation, labeling and hybridization, chip washing, and scanning were performed the same as for the DNA methylation assays.

The original scanned output CEL files were deposited into the Gene Expression Omnibus database with a series entry of GSE14620 (available at <http://www.ncbi.nlm.nih.gov/geo/query/acc.cgi?acc=GSE14620>). The CEL files were analyzed with Affymetrix tiling analysis software to generate binary analysis result (BAR) files that contain the intensities for all probes on the arrays. The intensities on each probe at each modification for each age were converted to -fold changes against the intensities of the related probe on the input chip from genomic DNA without immunoprecipitation. -Fold enrichment on each probe was estimated by using the Hodges-Lehmann estimator associated with the Wilcoxon rank sum test (see Tiling Analysis Software User Guide). The results were compiled into browser extensible data files. The three chromosome-wide browser extensible data files are presented in the Supplementary Materials.

Based on the Affymetrix's recommendation, thresholds for DNA methylation, H3K4me2, and H3K27me3 enrichment were set as 3-fold signal increases of immunoprecipitated signals versus nonimmunoprecipitated signals, which corresponds to a false discovery rate of less than 0.1. A genomic region with a sequence of >200 bp and an average signal increase greater than the threshold was defined as an enriched interval. A genomic region with one or more enriched intervals in close proximity to each other (at least one base overlap) at any given age was defined as an active region. Exact locations of an enriched interval or an active region along with its proximity to gene annotations and other genomic features were determined by Chip Analysis Software (Genepathway, San Diego, CA). The active regions within a gene margin, which is arbitrarily defined as 10,000 bp 5'- from the gene transcriptional start site to 10,000 bp from 3'-UTR end of the gene, were assigned to the associated gene. The overall -fold changes of each epigenetic modification in a gene were represented by average peak values of all active regions within margins of the associated genes.

**Quantification of Gene Expression Levels by bDNA or Reverse Transcriptase-Polymerase Chain Reaction.** mRNA levels of the *Cyp3a11*, *Cyp3a16*, *Cyp3a25*, *Cyp3a41b*, and *Gapdh* in liver cells at different ages were quantified by using branched DNA technology described previously (Hart et al., 2009). mRNA levels of the *Cdk8*, *Atp5j2*, and *Gapdh* genes were quantified by using custom Taqman gene expression assays (assay IDs Mm00731453\_s1, Mm00834769\_g1, and Mm99999915\_ml, respectively) with an ABI Prism 7900 Sequence Detection System (Applied Biosystems, Foster City, CA) following the manufacturer's protocol. -Fold changes of mRNA levels were calculated using the comparative Ct method according to the manufacturer's instruction.

## Results

**DNA Methylation Profiles along the *Cyp3a* Locus at Different Ages.** Epigenetic profiles of DNA methylation along the *Cyp3a* locus in livers of mice at different ages were determined by a combination of immunoprecipitation of methylated DNA with a specific antibody against 5-methylcytosine and hybridization of the precipitated DNA fragments to Affymetrix GeneChip Mouse Tiling 2.0R E Arrays.

Figure 2A shows DNA methylation signal enrichment (-fold changes over background) along the probes in a 1.37-Mb genomic region (Chr5:145,310,000–146,680,000) containing the *Cyp3a* gene cluster and its adjacent 5' and 3' domains.

Because of high similarity of DNA sequences within the *Cyp3a* locus, several genomic areas have signal gaps, including the *Cyp3a44* and *Cyp3a41a* regions between the *Cyp3a41b* and *Cyp3a11* genes. A total of 16 enriched intervals were identified (Supplementary Table S1.1), corresponding to four active regions at all ages (Supplementary Table S2.1). One of the active regions was located in an intergenic region between the *Cyp3a25* and *Cyp3a11* genes, but beyond the margin (see definition under *Materials and Methods*) of either gene. Two active regions were found in the gene regions of *Rnf6*

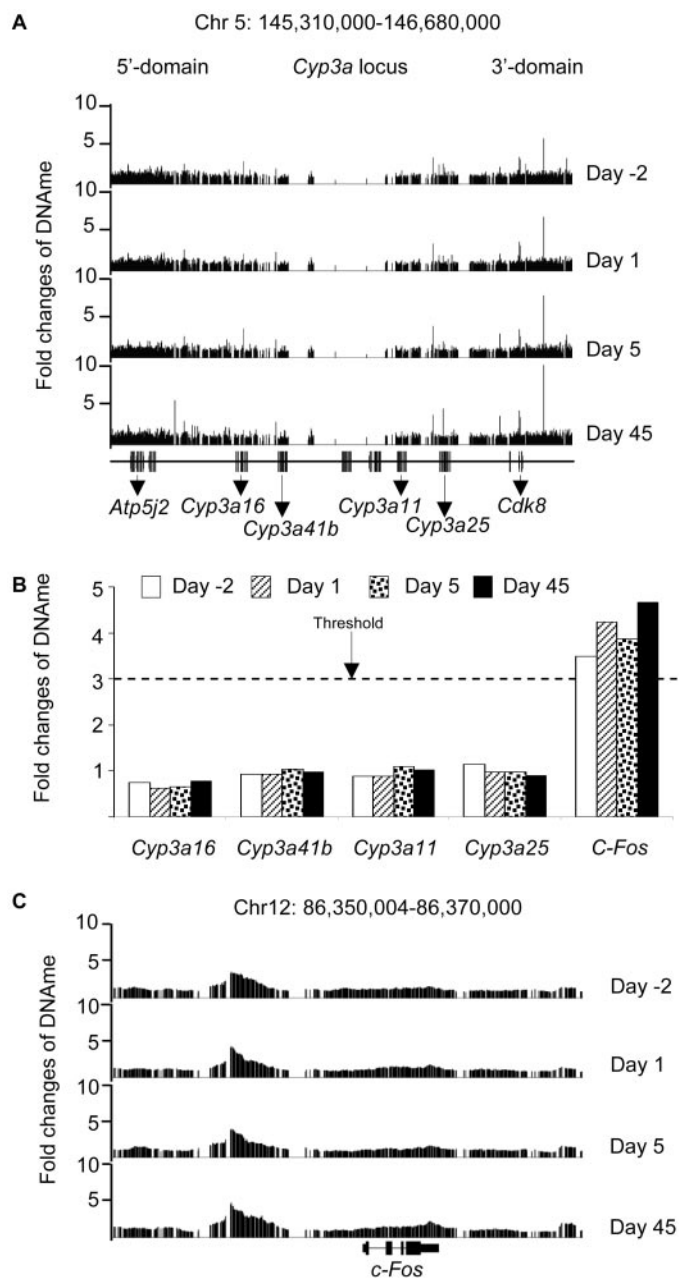


**Fig. 2.** Status of DNA methylation along the *Cyp3a* locus and its adjacent 5' and 3' domains during liver maturation. **A**, browser view of -fold changes of DNA methylation along the *Cyp3a* locus and its adjacent 5' and 3' domains in livers of mice at different ages. **B**, -fold enrichment of DNA methylation in the *Cyp3a* and *c-Fos* genes. The enrichment of DNA methylation was presented as the average -fold changes over background of all probes within the margins of the *Cyp3a* genes or the promoter of the *c-Fos* gene. **C**, browser view of -fold changes of DNA methylation along the *c-Fos* gene in livers of mice at different ages.

(3'-UTR) and *Cdk8* (Intron 4), respectively. The final active region was located in an intergenic region beyond the margin of the *Cdk8* gene. DNA sequences within the margins of *Cyp3a16*, *Cyp3a41b*, *Cyp3a11*, and *Cyp3a25* were not hypermethylated at any age (Fig. 2B and Table 1).

Enriched DNA methylation was found in the promoter of *c-Fos* gene on chromosome 12 at all ages (Fig. 2, B and C). This region has been reported to be methylated in mouse liver (Tao et al., 1999), which serves as a positive region for the DNA methylation assay.

**H3K4me2 Profiles along the *Cyp3a* Locus at Different Ages.** Epigenetic profiles of H3K4me2 along the *Cyp3a* locus in livers of mice at the four ages were determined by a combination of immunoprecipitation with a specific H3K4me2 antibody and hybridization of the immunoprecipitated DNA fragments to Affymetrix GeneChip Mouse Tiling 2.0R E Arrays. Figure 3A shows H3K4me2 signal enrichment (-fold changes over background) along the 1.37-Mb genomic region. A total of 98 H3K4me2-enriched intervals were identified in this region of DNA sequences in livers of mice at four ages, which are presented in Supplementary Table S1.2. Forty-three H3K4me2-active regions were found in this region, and the average peak values of each active region at different ages are presented in Supplementary Table S2.2.

Table 1 lists the overall -fold increases of H3K4me2 in the genes represented by average peak values of all active regions within margins of the associated genes. The data in Table 1 and Fig. 3 demonstrate that there are three distinct patterns of H3K4me2 modification through liver maturation in the four different chromatin domains. In Pattern I, consistent H3K4me2 enrichment was found in all ages in the adjacent 5' and 3' domains, containing numerous housekeeping genes, such as *Atp5j2* and *Cdk8*. In Pattern II, H3K4me2 enrichment increased from day -2 to days 1 and 5 and then decreased at day 45 in a chromatin domain containing the *Cyp3a16* and *Cyp3a41b* genes. The enriched peaks occurred around the TSS of the genes (see a detailed picture of *Cyp3a16* in Fig. S1A in the Supplementary Data). In Pattern III, H3K4me2 enrichment gradually increased from day -2, through days 1 and 5 to day 45 in a chromatin domain containing the *Cyp3a11* and *Cyp3a25* genes. The enriched peaks also occurred around the TSS of the genes (see a detailed image of *Cyp3a11* in Fig. S1B in the Supplementary Data). To determine the relationship between the H3K4me2 modification patterns and their ontogenic gene expression, we compared H3K4me2 enrichment levels within margins of the *Atp5j2*, *Cyp3a16*, *Cyp3a41b*, *Cyp3a11*, *Cyp3a25*, and *Cdk8* genes to their relative mRNA levels at different ages (Fig. 3B). The H3K4me2 alteration patterns are associated with their gene expression patterns without exception.

**H3K27me3 Profiles along the *Cyp3a* Locus at Different Ages.** A strategy similar to that used for H3K4me2 was applied to establish the H3K27me3 modification profiles. Figure 4A shows the signal enrichment of H3K27me3 along the 1.37-Mb genomic region in livers of mice at the four ages. A total of 19 H3K27me3-enriched intervals (see Supplementary Table S1.3) were identified in this genomic region. Each interval formed a unique active region (Supplementary Table S2.3). Two patterns were observed (Table 1 and Fig. 4). In Pattern I, no H3K27me3 enrichment was found at any age in the adjacent 5', and 3' domains as well as the *Cyp3a11*

**TABLE 1**  
Epigenetic modifications during mouse liver maturation in the 1.37-Mb genomic region containing the *Cyp3a* locus and adjacent 5' and 3' domains  
The presented data are the average peak values of all active regions within margins of the genes. Boldface type indicates the peak values higher than the thresholds.

	Chromatin Domains and Genes in Those Domains											
	5' Domain			<i>Cyp3a16/Cyp3a41b</i>			<i>Cyp3a11/Cyp3a25</i>			3' Domain		
	<i>Aryc1a</i>	<i>Pdap1</i>	<i>Atp5j2</i>	<i>Zfp99</i>	<i>Zfp655</i>	<i>Cyp3a16</i>	<i>Cyp3a41b</i>	<i>Cyp3a11</i>	<i>Cyp3a25</i>	<i>Raf6</i>	<i>Cdk8</i>	
Gene length (bp)	24,887	13,856	14,816	19,491	31,871	7886	16,506	15,547	33,385	25,247	32,391	
No. intervals	4	9	14	6	12	11	13	2	3	12	38	
No. active regions	1	3	5	3	4	10	12	2	3	3	14	
Position of active regions	In gene	In gene	In gene	In gene & upstream	In gene & upstream	In gene & upstream	In gene & upstream	In gene	Upstream	In gene & upstream	In gene & upstream	
DNAme												
Day -2	1.22	1.16	1.28	1.28	1.16	0.75	0.93	0.88	1.15	3.35	5.66	
Day 1	1.32	1.08	1.17	1.17	1.24	0.63	0.93	0.88	0.98	3.62	6.75	
Day 5	1.36	1.09	1.17	1.17	1.22	0.65	1.03	1.10	0.98	3.52	7.78	
Day 45	1.46	0.94	1.12	1.12	1.19	0.78	0.97	1.02	0.90	4.22	12.9	
H3K4me2												
Day -2	7.41	4.33	6.52	5.52	4.42	1.37	0.97	1.36	1.19	5.38	3.76	
Day 1	6.58	4.20	5.81	4.75	4.40	3.49	3.08	2.21	1.59	5.82	3.43	
Day 5	6.79	4.40	5.71	4.69	4.50	3.39	3.05	2.53	2.17	5.61	3.54	
Day 45	5.95	3.30	4.80	3.72	4.94	1.26	1.28	5.16	4.31	5.07	4.14	
H3K4me2 pattern			I					III			I	
H3K27me3												
Day -2	1.21	0.88	1.16	1.16	1.23	0.90	0.84	1.04	1.25	1.37	1.16	
Day 1	1.26	0.94	1.20	1.20	1.17	0.86	0.83	0.93	1.04	1.26	1.14	
Day 5	1.40	0.93	1.20	1.20	1.21	0.86	0.82	0.91	0.99	1.21	1.12	
Day 45	1.22	0.89	1.03	1.03	1.04	3.83	4.65	0.85	1.02	1.13	1.05	
H3K27me3 pattern			I			II		I			I	

*Cyp3a25* domain. In Pattern II, H3K27me3 was enriched at only day 45 in the *Cyp3a16/Cyp3a41b* domain. The enriched peaks were observed in the entire gene and 5' upstream of *Cyp3a16* or *Cyp3a41b* (see a detailed picture of *Cyp3a16* in Fig. S1C in the Supplementary Data). Gene expression levels of *Cyp3a16* and *Cyp41b* were almost undetectable at day 45 (Fig. 3B).

The results of DNA and histone methylation were obtained with a single pool of livers analyzed on a single tiling array. The data obtained by the ChIP-on-chip assays were further validated by ChIP quantitative real-time PCR in mouse liver samples (three replicates) in the selected genomic or gene regions (see Supplementary Information and Fig. S2). Data generated by ChIP real-time PCR agreed with the results established by the ChIP-on-chip assays.

## Discussion

Epigenetic profiles of DNA methylation along the *Cyp3a* locus and its adjacent 5' and 3' domains during liver maturation have been established by using ChIP-on-chip assays with an antibody against 5-methyl-cytosine. Although this method cannot resolve DNA methylation at base pair resolution as shotgun bisulphate sequencing does (Cokus et al., 2008), it has been used for ultrasensitive detection and genome-wide high-resolution mapping of DNA methylation (Pröll et al., 2006; Zhang et al., 2006). Two active regions of DNA methylation were identified in the *Rnf6* and *Cdk8* genes, but the contribution of DNA methylation on regulation of their gene expression needs to be determined. However, the current study shows that DNA methylation may not

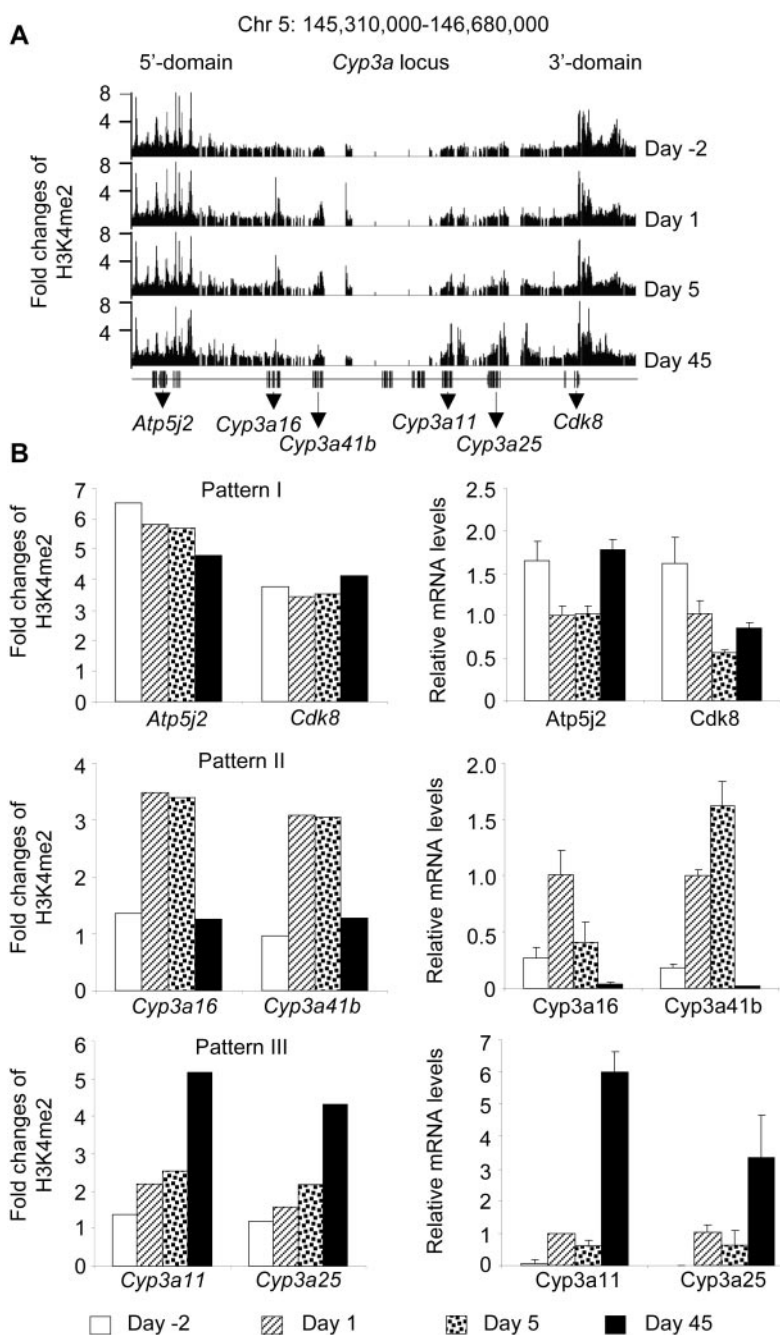


**Fig. 3.** Association between H3K4me2 enrichment levels and transcription levels of the *Cyp3a* genes and two adjacent housekeeping genes during liver maturation. A, browser view of H3K4me2 -fold changes along the *Cyp3a* locus and its adjacent 5' and 3' domains in livers of mice at different ages. B, comparison between H3K4me2 alteration patterns and expression patterns of the *Atp5j2*, *Cyp3a16*, *Cyp3a41b*, *Cyp3a11*, *Cyp3a25*, and *Cdk8* genes in livers of mice at different ages. H3K4me2 -fold changes are presented as the average peak values of all active regions within the margins of the target genes. mRNA levels of each individual gene were quantified by branched DNA technology or TaqMan real-time PCR and then normalized to the levels of *Gapdh* and shown as relative levels to day 1. Bars represent the mean  $\pm$  S.D. from five individual samples.

play a role in the regulation of ontogenic Cyp3a transcription, because levels of DNA methylation are consistently low in the *Cyp3a* genes across all ages (Fig. 2B).

Epigenetic profiles of H3K4me2 and H3K27me3 along the Cyp3a locus and its adjacent 5' and 3' domains during liver maturation have also been established by using ChIP-on-chip assays with verification by ChIP real-time PCR. Alterations of H3K4me2 and H3K27me3 are associated to the ontogenic expression of the *Cyp3a* genes. Four different chromatin domains with three distinct H3K4me2 and H3K27me3 alteration patterns were found during liver maturation in the 1.37-Mb genomic region at the distal end of chromosome 5 (Fig. 5).

In pattern I of Fig. 5, the adjacent 5' and 3' domains of the *Cyp3a* locus are consistently methylated at H3K4 in livers of mice across all ages. Histone methylation is an epigenetic modification that influences chromatin configuration and higher-order chromatin structure by affecting interactions between histone and DNA or between different histones (Bártová et al., 2008). Methylation at H3K4 normally results in an open chromatin configuration and is therefore associated with the activation of gene transcription. Numerous housekeeping genes are located in the adjacent 5' and 3' domains of the *Cyp3a* locus, such as *Atp5j2* and *Cdk8*. Their consistent expression is essential for cellular functions during development. For example, *Cdk8* is a kinase subunit of the mediator complex linked with basal transcriptional machinery and involved in regulation of gene transcription and cell cycle progress (Furumoto et al., 2007). *Cdk8* is essential for embryogenesis, because *Cdk8*<sup>-/-</sup>

mice are embryonic lethal (Westerling et al., 2007). Consistent H3K4 methylation in the adjacent 5' and 3' domains of the *Cyp3a* locus may be responsible for keeping these chromatin domains open for stable expression of the housekeeping genes during liver maturation.

In pattern II of Fig. 5, both H3K4me2 and H3K27me3 in the chromatin domain containing the *Cyp3a16* and *Cyp3a41b* genes are changed during liver maturation. Although the functions of the Cyp3a16 and Cyp3a41 proteins are unclear in livers of mice, it has been known that *Cyp3a16* is only expressed in neonatal liver, not in adult liver (Itoh et al., 1997; Nakayama et al., 2001; Hart et al., 2009). Some studies reported that Cyp3a16 is expressed in adult female liver at a much higher level than in adult male liver (Holloway et al., 2007). Cyp3a41 is a female-specific Cyp3a enzyme, which is not expressed in adult male liver (Sakuma et al., 2000; Hart et al., 2009). These enzymes may have some protective roles in neonatal livers just as the human fetal-specific CYP3A7, which is involved in the production of 16 $\alpha$ -OH-DHEA-sulfate (a precursor of placental estriol synthesis) and serves a protective role by preventing the accumulation of excess retinoid and DHEA-sulfate in fetal livers (Chen et al., 2000). The current study shows that increases of H3K4me2 in margins of the *Cyp3a16* and *Cyp3a41b* genes are found in mouse livers during neonatal ages (days 1 and 5), which are associated with increased gene expression in livers of mice at these ages. Furthermore, increases of H3K27me3 are found in the margins of *Cyp3a16* and *Cyp3a41b* genes in livers of mice at only 45 days of age. Enrichment of H3K27me3 in promoters and gene-bodies has been associated with inactivation of gene transcription (Lan et al., 2007; Swigut and Wysocka, 2007). Thus, increases of H3K27me3 in the chromatin domain containing both *Cyp3a16* and *Cyp3a41b* may link to suppression of their gene expression. H3K4me2 and H3K27me3 have opposing roles in controlling gene expression. Decreases of H3K4me2 and increases of H3K27me3 within the margins of the *Cyp3a16* and *Cyp3a41b* genes may be responsible for

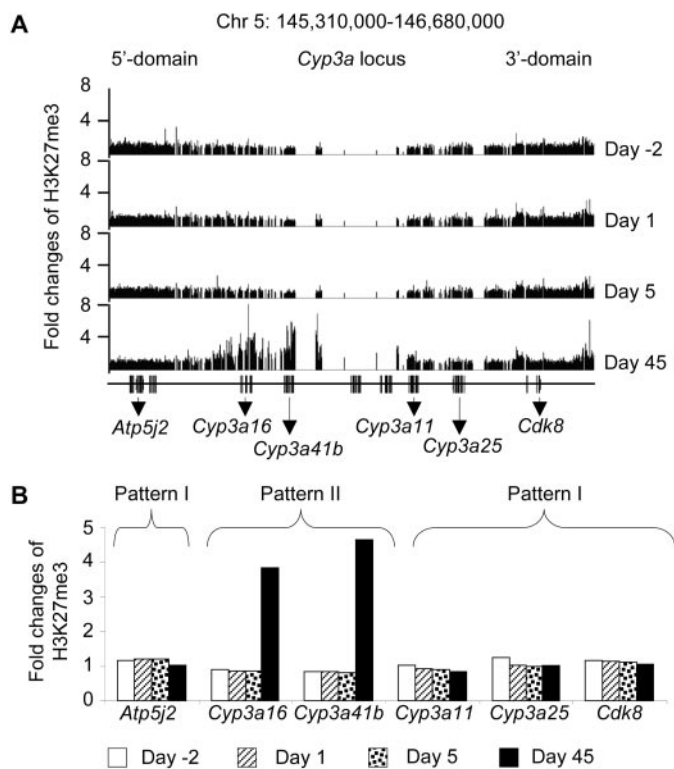


**Fig. 4.** Association between H3K27me3 alteration and *Cyp3a* gene expression during liver maturation. A, browser view of H3K27me3 -fold changes along the *Cyp3a* locus and its adjacent 5' and 3' domains in livers of mice at different ages. B, H3K27me3 alterations in the *Cyp3a16* and *Cyp3a41b* genes in livers of mice at different ages. H3K27me3 -fold changes are presented as the average peak values of all active regions within the margins of the *Cyp3a16* and *Cyp3a41b* genes.

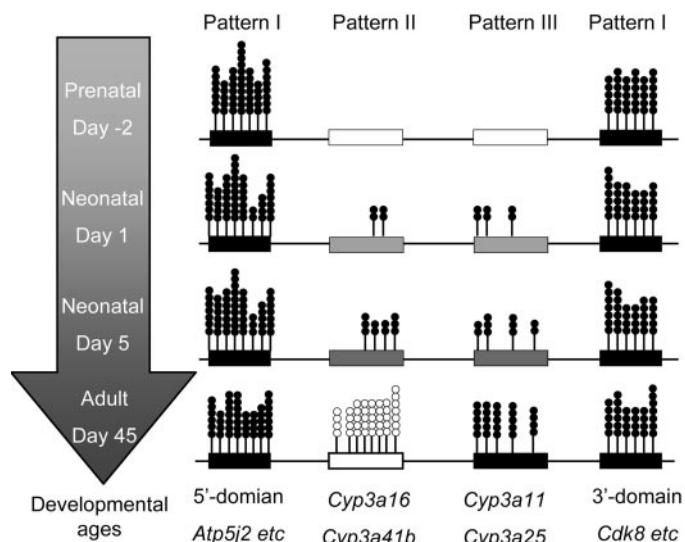


**Fig. 5.** Patterns of dynamic changes of H3K4me2 and H3K27me3 along the *Cyp3a* locus and its adjacent 5' and 3' domains during liver maturation. Bars indicate different chromatin domains with different histone modification patterns. A small closed or open circle represents a 1-fold increase of H3K4me2 or H3K27me3, respectively, at the associated positions.

switching off their gene expression in livers of adult mice. The switch of histone modification levels between H3K4me2 and H3K27me3 has been also identified in regulation of *Hox* genes in response to certain developmental and environmental cues (Schuettengruber et al., 2007; Iimura and Pourquié, 2007) and in the *Bmp-2* gene in response to an inflammatory stimulus (De Santa et al., 2007).

In pattern III of Fig. 5, levels of H3K4me2 gradually increase from prenatal, through neonatal, to adult ages in the chromatin domain containing *Cyp3a11* and *Cyp3a25*. Liver has a functional transition from a hematopoietic organ before birth to a major metabolic and detoxification organ after birth (Hata et al., 2007). Some xenobiotic-metabolizing enzymes have ontogenic expression patterns, which are expressed at low levels before birth, gradually increase after birth, and reach high levels in adults. *Cyp3a11* and *Cyp3a25* are the P450-metabolizing enzymes in mouse liver with such an ontogenic expression pattern (Hart et al., 2009). The current study provides evidence showing that the expression levels of *Cyp3a11* and *Cyp3a25* at different ages are associated with the levels of H3K4 methylation in the margins of *Cyp3a11* and *Cyp25* genes. Increases of H3K4me2 around these *Cyp3a* genes during liver development may be responsible for switching on their gene expression after birth. In agreement with reports from other genes (De Santa et al., 2007; Iimura and Pourquié, 2007; Saleh et al., 2008), these data support a conclusion that histone methylation plays a role in regulating gene transcription in a locus-specific and dynamic manner to satisfy physiological needs during development.

Methylation and demethylation of H3K4 and H3K27 are driven by specific histone methyltransferases and demethylases. Several histone modification enzymes have been identified (Cho et al., 2007; Issaeva et al., 2007). H3K27 demethylase, UTX, a JmjC-domain protein, is reported to be associated with two H3K4 methyltransferases of the MLL family, MLL3 and MLL4 in a core complex protein (Issaeva et al., 2007). Another H3K27 demethylase, JMJD3, coimmunoprecipitates with the core complex component containing H3K4 methyltransferases (Cho et al., 2007). These findings may suggest that association of H3K27 demethylases with H3K4 methyltransferases may be a general phenomenon for switching on/off gene expression at different developmental stages. Identification of specific methyltransferases and demethylases for H3K4 and H3K27 is a next step toward understanding the mechanisms responsible for the developmental switch between *Cyp3a11* and *Cyp3a16*.

The association between *Cyp3a* expression and histone modifications is also observed in other tissues with tissue-specific patterns. For example, genome-wide status of chromatin modifications has been established in pluripotent and lineage-committed cells, including brain (Mikkelsen et al., 2007). Using the data generated by Mikkelsen et al. (2007), Fig. S3 in the supplementary data shows H3K4me2 and H3K27me3 along the *Cyp3a* locus in brain. *Cyp3a* genes are not expressed in brain, but its adjacent housekeeping genes, such as *Atp5j2*, *Rnf6*, and *Cdk8*, are expressed. *Atp5j2*, *Rnf6* and *Cdk8*, but not *Cyp3a* genes, are enriched for H3K4me2 in brain. Furthermore, the *Cyp3a11* and *Cyp3a16* genes are enriched for H3K27me3.

In conclusion, the present study demonstrates that alterations of H3K4me2 and H3K27me3 are locus-specific with

different patterns at different chromatin domains. The patterns of H3K4me2 and H3K27me3 modifications are associated with the patterns of ontogenic expression of the *Cyp3a* genes during liver maturation. Switching on expression of the *Cyp3a16* and *3a41b* gene in neonatal livers and *Cyp3a11* and *3a25* in adult livers seems to be due to increases of H3K4me2 around the related genes. Switching off expression of the *Cyp3a16* and *3a41b* genes in adult livers seems to be due to decreases of H3K4me2 and increases of H3K27me3 around the related genes.

#### Acknowledgments

We thank Drs. Kenneth Peterson and Patrick Fields for their advice on the experimental design, Dr. Partha Krishnamurthy for critical reading of the manuscript, and Kaori Nakamoto for technical support.

#### References

- Bártová E, Krejčí J, Harnicarová A, Galiová G, and Kozubek S (2008) Histone modifications and nuclear architecture: a review. *J Histochem Cytochem* **56**:711–721.
- Bird A (2002) DNA methylation patterns and epigenetic memory. *Genes Dev* **16**:6–21.
- Chen H, Fantel AG, and Juchau MR (2000) Catalysis of the 4-hydroxylation of retinoic acids by *cyp3a7* in human fetal hepatic tissues. *Drug Metab Dispos* **28**:1051–1057.
- Cho YW, Hong T, Hong S, Guo H, Yu H, Kim D, Guszczynski T, Dressler GR, Copeland TD, Kalkum M, et al. (2007) PTIP associates with MLL3 and MLL4-containing histone 3 lysine 4 methyltransferase complex. *J Biol Chem* **282**:20395–20406.
- Cokus SJ, Feng S, Zhang X, Chen Z, Merriman B, Haudenschild CD, Pradhan S, Nelson SF, Pellegrini M, and Jacobsen SE (2008) Shotgun bisulphate sequencing of the Arabidopsis genome reveals DNA methylation patterning. *Nature* **452**:215–219.
- De Santa F, Totaro MG, Prosperini E, Notarbartolo S, Testa G, and Natoli G (2007) The histone H3 lysine-27 demethylase Jmjd3 links inflammation to inhibition of polycomb-mediated gene silencing. *Cell* **130**:1083–1094.
- Esteller M (2007) Cancer epigenomics: DNA methylomes and histone-modification maps. *Nat Rev Genet* **8**:286–298.
- Feinberg AP (2007) Phenotypic plasticity and the epigenetics of human disease. *Nature* **447**:433–440.
- Furumoto T, Tanaka A, Ito M, Malik S, Hirose Y, Hanaoka F, and Ohkuma Y (2007) A kinase subunit of the human mediator complex, CDKS, positively regulates transcriptional activation. *Genes Cells* **12**:119–132.
- Hart SN, Cui Y, Klaassen CD, and Zhong XB (2009) Three patterns of cytochrome P450 gene expression during liver maturation in mice. *Drug Metab Dispos* **37**:116–121.
- Hata S, Namae M, and Nishina H (2007) Liver development and regeneration: from laboratory study to clinical therapy. *Dev Growth Differ* **49**:163–170.
- Heintzman ND, Stuart RK, Hon G, Fu Y, Ching CW, Hawkins RD, Barrera LO, Van Calcar S, Qu C, Ching KA, et al. (2007) Distinct and predictive chromatin signatures of transcriptional promoters and enhancers in the human genome. *Nat Genet* **39**:311–318.
- Hines RN (2008) The ontogeny of drug metabolism enzymes and implications for adverse drug events. *Pharmacol Ther* **118**:250–267.
- Holloway MG, Cui Y, Laz EV, Hosui A, Hennighausen L, and Waxman DJ (2007) Loss of sexually dimorphic liver gene expression upon hepatocytes-specific deletion of Stat5a-Stat5b locus. *Endocrinology* **148**:1977–1986.
- Iimura T and Pourquié O (2007) Hox genes in time and space during vertebrate body formation. *Dev Growth Differ* **49**:265–275.
- Issaeva I, Zonis Y, Rozovskaia T, Orlovsky K, Croce CM, Nakamura T, Mazo A, Eisenbach L, and Canaani E (2007) Knockdown of ALR (MLL2) reveals ALR target genes and leads to alteration in cell adhesion and growth. *Mol Cell Biol* **27**:1889–1903.
- Itoh S, Abe Y, Kubo A, Okuda M, Shimoji M, Nakayama K, and Kamataki T (1997) Isolation of a promoter region in mouse cytochrome P450 3A (*Cyp3A16*) gene and its transcriptional control. *Biochim Biophys Acta* **1350**:155–158.
- Kiefer JC (2007) Epigenetics in development. *Dev Dyn* **236**:1144–1156.
- Kouzarides T (2007) Chromatin modifications and their function. *Cell* **128**:693–705.
- Lacroix D, Sonnier M, Moncion A, Cheron G, and Creteil T (1997) Expression of CYP3A in the human liver—evidence that the shift between CYP3A7 and CYP3A4 occurs immediately after birth. *Eur J Biochem* **247**:625–634.
- Lan F, Bayliss PE, Rinn JL, Whetstone JR, Wang JK, Chen S, Iwase S, Alpatov R, Issaeva I, Canaani E, et al. (2007) A histone H3 lysine 27 demethylase regulates animal posterior development. *Nature* **449**:689–694.
- Leeder JS, Gaedigk R, Marcucci KA, Gaedigk A, Vyhldal CA, Schindel BP, and Pearce RE (2005) Variability of CYP3A7 expression in human fetal liver. *J Pharmacol Exp Ther* **314**:626–635.
- Mikkelsen TS, Ku M, Jaffe DB, Issac B, Lieberman E, Giannoukos G, Alvarez P, Brockman W, Kim TK, Koche RP, et al. (2007) Genome-wide maps of chromatin state in pluripotent and lineage-committed cells. *Nature* **448**:553–560.
- Nakayama K, Sudo Y, Sasaki Y, Iwata H, Takahashi M, and Kamataki T (2001)

- Studies on transcriptional regulation of Cyp3a16 gene in mouse livers by application of direct DNA injection method. *Biochem Biophys Res Commun* **287**:820–824.
- Nan X, Ng HH, Johnson CA, Laherty CD, Turner BM, Eisenman RN, and Bird A (1998) Transcriptional repression by the methyl-CpG-binding protein MeCP2 involves a histone deacetylase complex. *Nature* **393**:386–389.
- O'Geen H, Nicolet CM, Blahnik K, Green R, and Farnham PJ (2006) Comparison of sample preparation methods for ChIP-chip assay. *Biotechniques* **41**:577–580.
- Pröll J, Fördermayr M, Wechselberger C, Pammer P, Sonnleitner M, Zach O, and Lutz D (2006) Ultra-sensitive immunodetection of 5'-methyl cytosine for DNA methylation analysis on oligonucleotide microarrays. *DNA Res* **13**:37–42.
- Reik W (2007) Stability and flexibility of epigenetic gene regulation in mammalian development. *Nature* **447**:425–432.
- Robertson KD (2005) DNA methylation and human disease. *Nat Rev Genet* **6**:597–610.
- Saleh A, Alvarez-Venegas R, and Avramova Z (2008) Dynamic and stable histone H3 methylation patterns at the Arabidopsis FLC and AP1 loci. *Gene* **423**:43–47.
- Sakuma T, Takai M, Endo Y, Kuroiwa M, Ohara A, Jarukamjorn K, Honma R, and Nemoto N (2000) A novel female-specific member of the CYP3A gene subfamily in the mouse liver. *Arch Biochem Biophys* **377**:153–162.
- Schuettengruber B, Chourrout D, Vervoort M, Leblanc B, and Cavalli G (2007) Genome regulation by polycomb and trithorax proteins. *Cell* **128**:735–745.
- Schuetz JD, Beach DL, and Guzelian PS (1994) Selective expression of cytochrome P450 CYP3A mRNAs in embryonic and adult human liver. *Pharmacogenetics* **4**:11–20.
- Sim SC, Edwards RJ, Boobis AR, and Ingelman-Sundberg M (2005) CYP3A7 protein expression is high in a fraction of adult human livers and partially associated with the CYP3A7\*1C allele. *Pharmacogenet Genomics* **15**:625–631.
- Stevens JC (2006) New perspectives on the impact of cytochrome P450 3A expression for pediatric pharmacology. *Drug Discov Today* **11**:440–445.
- Stevens JC, Hines RN, Gu C, Koukouritaki SB, Manro JR, Tandler PJ, and Zaya MJ (2003) Developmental expression of the major human hepatic CYP3A enzymes. *J Pharmacol Exp Ther* **307**:573–582.
- Swigut T and Wysocka J (2007) H3K27 demethylases, at long last. *Cell* **131**:29–32.
- Tao L, Ge R, Xie M, Kramer PM, and Pereira MA (1999) Effect of trichloroethylene on DNA methylation and expression of early-intermediate protooncogenes in the liver of B6C3F1 mice. *J Biochem Mol Toxicol* **13**:231–237.
- Wang Z, Zang C, Rosenfeld JA, Schones DE, Barski A, Cuddapah S, Cui K, Roh TY, Peng W, Zhang MQ, et al. (2008) Combinatorial patterns of histone acetylations and methylations in the human genome. *Nat Genet* **40**:897–903.
- Westerling T, Kuuluvainen E, and Mäkelä TP (2007) Cdk8 is essential for preimplantation mouse development. *Mol Cell Biol* **27**:6177–6182.
- Wilkinson GR (2005) Drug metabolism and variability among patients in drug response. *N Engl J Med* **352**:2211–2221.
- Williams JA, Ring BJ, Cantrell VE, Jones DR, Eckstein J, Ruterbories K, Hamman MA, Hall SD, and Wrighton SA (2002) Comparative metabolic capabilities of CYP3A4, CYP3A5, and CYP3A7. *Drug Metab Dispos* **30**:883–891.
- Zhang X, Yazaki J, Sundaresan A, Cokus S, Chan SW, Chen H, Henderson IR, Shinn P, Pellegrini M, Jacobsen SE, et al. (2006) Genome-wide high-resolution mapping and functional analysis of DNA methylation in Arabidopsis. *Cell* **126**:1189–1201.

**Address correspondence to:** Dr. Xiao-bo Zhong, Department of Pharmacology, Toxicology, and Therapeutics, The University of Kansas Medical Center, 3901 Rainbow Boulevard, Kansas City, KS 66160. E-mail: xzhong@kumc.edu